Exploring bacteria–surface interactions with a fluorescent membrane tension probe

M.C. Gonzalez-Garcia, D. Ballesteros, J.J. Hernández, M. Pazos, I. Rodríguez, J. Requejo-Isidro, & C. Flors

Exploring bacteria-surface interactions with a fluorescent membrane tension probe

*M. Carmen González-García,[1] Daniel Ballesteros,[2] Jaime J. Hernández,[1¶] Manuel Pazos,[2,3] Isabel Rodríguez,[1] Jose Requejo-Isidro,[4,5] Cristina Flors[1,4]**

[1]Madrid Institute for Advanced Studies in Nanoscience (IMDEA Nanociencia), C/ Faraday 9, Madrid 28049, Spain

[2]Centro de Biología Molecular Severo Ochoa (CBMSO) CSIC - Universidad Autónoma de Madrid C/ Nicolás Cabrera 1, Madrid 28049, Spain.

[3]Instituto Universitario de Biología Molecular (IUBM) y Departamento de Biología Molecular, Universidad Autónoma de Madrid, Madrid, Spain.

[4]Nanobiotechnology Unit Associated to the National Center for Biotechnology (CNB-CSIC-IMDEA), C/ Faraday 9, Madrid 28049, Spain

[5]Centro Nacional de Biotecnología (CNB-CSIC), C/ Darwin 3, Madrid 28049, Spain

CLASSIFICATION: Biological Sciences/Biophysics and Computational Biology; Physical Sciences/Applied Physical Sciences

KEYWORDS: bacteria, cell-material interface, Flipper-TR, fluorescence lifetime imaging, membrane tension probe, nanotopography.

ABSTRACT

Understanding how bacteria interact with surfaces is critical for advancing applications in biofilm and biofouling prevention, biomaterial development or biosensing. However, the biophysical mechanisms underlying these interactions remain poorly characterized, and novel microscopy strategies are needed to specifically address the biointerface. In this study, we employ fluorescence lifetime imaging microscopy (FLIM) with the mechanosensitive probe Flipper-TR to investigate membrane tension in live bacteria interacting with various surfaces. We show that Flipper-TR stains both Gram-positive and Gram-negative bacterial membranes, exhibiting fluorescence lifetimes shorter than those in eukaryotic cells, with slight variations between bacterial types and likely reflecting differences in membrane composition. Flipper-TR displays lifetime variations along the vertical axis of bacterial cells, suggesting spatial differences in membrane tension influenced by cell wall architecture. Our results further demonstrate that Flipper-TR is responsive to the nature of bacterial interactions with surfaces. By comparing bacterial immobilization on surfaces with different coatings, we show that Flipper-TR can sensitively distinguish differences in membrane tension arising from distinct adhesion mechanisms. Additionally, Flipper-TR detects changes in membrane tension when bacteria are exposed to engineered nanostructured substrates. Overall, this work offers new tools to study the mechanical aspects of bacterial-material interactions and contributes to providing design rules for novel materials that influence bacterial behavior.

SIGNIFICANCE

In natural environments, bacteria are primarily found attached to surfaces rather than as free-swimming cells. Their behavior is influenced by surface-specific mechanics such as hydrodynamic and adhesive forces, and the material properties of the surface. However, the biophysical mechanisms underlying bacterial-surface interactions, which can have a profound effect on bacterial physiology, remain poorly understood. In this study, we employ a mechanosensitive fluorescent probe to visualize and quantify the mechanical stress on bacterial membranes upon contact with a surface, and show that this method is sensitive enough to distinguish surfaces with different adhesive and topographical properties. This work expands the toolbox to study how physical forces influence bacteria and contributes to providing design rules for novel materials that modulate bacterial behavior.

INTRODUCTION

Understanding the way bacteria interact with surfaces is crucial in various fields, including biofouling, biofilm formation, biosensing and the development of antimicrobial materials.[1-4] However, fundamental aspects of the interaction between live bacteria and surfaces are poorly understood, such as what are the surface properties sensed by bacteria, or the molecular mechanisms for surface sensing and their biochemical responses. From the point of view of materials engineering, determining how to modulate surface properties to provoke a desired cellular response, including changes in morphology, alterations in metabolism or cell death, is of key importance.[1] Yet, there are challenges associated to the characterization of the interaction between surfaces and live bacteria in a biologically-relevant environment.[5] New microscopy tools specifically tailored to the cell-material interface can have a real impact on guiding the development of new classes of materials that inhibit or promote bacterial growth, and complement studies of the physiology of bacteria in contact with surfaces.[1,2,6-10]

We have previously reported the use of advanced microscopy methods to understand bacterial-material interaction in live cells,[11-13] mostly in the context of mechano-bactericidal nanomaterials. The latter exert antimicrobial effects through purely physical mechanisms and hold promise as alternative strategies to traditional antibiotics for combating bacterial infection while avoiding the development of resistance.[14-16] Herein, we focus on understanding the effects of surface properties on bacterial membranes in living cells. To that end, we use the fluorescent probe Flipper-TR, a mechanosensitive push-pull fluorophore that inserts into membranes and whose lifetime reports on lateral forces (Figure S1).[17-19] This probe is composed by two dithienothiophene moieties that are twisted out of coplanarity in the ground state and that can be planarized under the application of compressive forces, leading to an increase in emission

efficiency and lifetime. Flipper-TR exhibits a double exponential fluorescence decay, although only the longer lifetime (which we refer to as τ_1, see below) is mechanosensitive.[17] The probe is therefore employed in fluorescence lifetime imaging microscopy (FLIM), in which image contrast is generated by changes in fluorescence lifetime rather than intensity. The fluorescence lifetime is the average time the fluorophore remains in the excited state after excitation, and is defined as the inverse sum of the radiative (k_r) and non-radiative (k_{nr}) rate constants. As the fluorescence lifetime does not depend on fluorophore concentration, absorption/scattering by the sample, photo-bleaching and/or excitation intensity, FLIM is more robust than intensity based methods and the technique of choice for sensing applications.[20,21]

One challenge with the use of Flipper-TR is that local changes in lipid composition, which in turn affect lipid packing, also alter its fluorescence lifetime. While this is typically not an issue for single phase membranes *in vitro*, interpretation of changes in fluorescence lifetime of Flipper-stained cell membranes remains challenging.[18,22] Therefore, we first establish its use in both Gram positive and Gram negative bacteria in FLIM experiments, since Flipper-TR has mostly been used in mammalian cells and few reports include bacteria.[18,23-25] We show that this probe is suitable for model systems representing both bacterial types, and is sensitive enough to discriminate bacterial contact with different surfaces, including mechano-bactericidal nanotopographies. Moreover, by using an additional solvatochromic probe that is environmentally sensitive but does not report on mechanical effects, we disentangle physical membrane stretching or compression from changes in lipid composition.

RESULTS AND DISCUSSION

Flipper-TR discriminates between bacterial membranes

We first compared Flipper-TR staining of Gram positive and negative bacteria using *Bacillus subtilis* 168 and *Escherichia coli* BW25113, respectively. Previous reports on *B. subtilis* show that the lifetime (τ_1) of Flipper-TR is well below 5 ns,[18,23-25] in comparison with the longer lifetime values up to 6 ns for eukaryotic cells and other organisms, and therefore it is reasonable to use a 80 MHz laser (that results in a 12.5 ns window) for these experiments.[18] Figures 1 and S2 show FLIM images, lifetime histograms and fluorescence decay curves for both model bacteria immobilized on CellTak, a polyphenolic adhesive protein typically used in microscopy experiments, and stained with 2 μM of the probe. Figure 1A shows clear membrane staining for both *B. subtilis* and *E. coli*. In *B. subtilis*, Flipper-TR in the poles and septal regions shows a longer lifetime than in the rest of the cell membrane, consistent with previous observations.[23] Besides mechanical effects, this longer lifetime may reflect different lipid compositions, especially in the septum.[26,27] The fluorescence lifetime distribution for *B. subtilis* is centered at 3.22 ± 0.16 ns, similar to previously reported values.[18,23] For *E. coli*, we find a slightly shorter Flipper-TR fluorescence lifetime of 3.05 ± 0.21 ns. The FLIM images show clear staining of the cell boundary in *E. coli*, supporting that Flipper-TR is indeed incorporated into the membrane.[28] Moreover, Figure S3 shows that, in both bacterial strains we have studied, the fluorescence signal at the membrane is well above autofluorescence, the latter with a much shorter fluorescence lifetime. To investigate further Flipper-TR localization in *E. coli*, whose cell wall is

more complex and includes an outer and inner (or cytoplasmic) membrane separated by a peptidoglycan layer, plasmolysis experiments were conducted (Figure S4). These experiments consist on specifically disrupting the bacterial inner membrane upon osmotic shock.[29] Flipper-TR fluorescence after plasmolysis was compared with that of the membrane probe FM 4-64, which is known to selectively stain the bacterial outer membrane.[26,29] Figure S2 shows very distinct fluorescence signal localization of Flipper-TR compared to FM 4-64, strongly suggesting that Flipper-TR traverses the outer membrane of Gram negative bacteria.

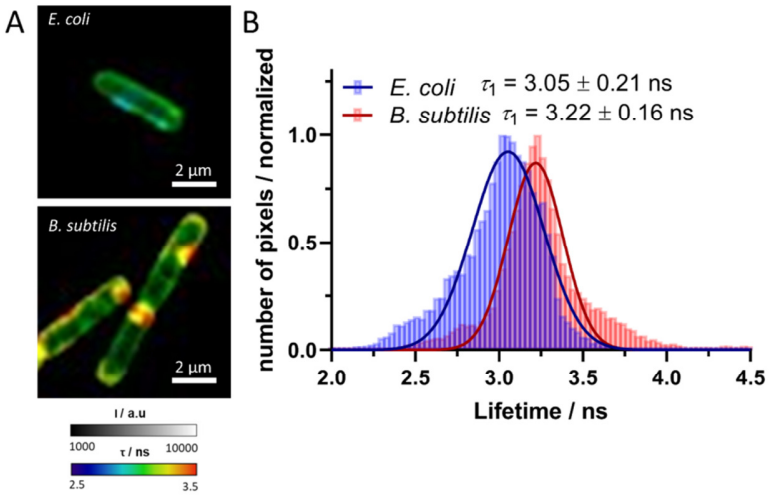

Figure 1. A) Overlaid intensity and FLIM images and B) fluorescence lifetime histograms of *E. coli* and *B. subtilis* stained with Flipper-TR at 2 µM and immobilized on CellTak (n>100 cells). τ_1 corresponds to the long lifetime in the biexponential decay.

Our observations suggest that Flipper-TR staining is suitable for both Gram positive and negative bacteria, showing slightly different fluorescence lifetime values, and in both cases significantly shorter than those observed in mammalian cells, as discussed above. The variation

in lifetime between membranes in both bacterial models may correspond, at least in part, to differences in membrane composition and do not necessarily reflect distinct membrane tension.

Membrane tension varies across bacterial height

In the FLIM experiments discussed in the previous section, the bacterial midplane was optically selected. An optical section of 0.9 µm was used to maximize photon acquisition, which is relatively thick compared to the bacterial height (1-2 µm) and therefore the imaged planes may contain fluorescence signal from a significant part of the bacterial cell. Since it has been previously shown that Flipper-TR exhibits different fluorescent lifetimes along cell height in eukaryotic cells, with shorter values at the basal plane compared to the apical plane,[18] we investigated if height-dependent fluorescence lifetimes also occur in bacteria. This is particularly relevant to our experiments, as we are interested in studying the cell-material interface. Therefore, several optical sections were acquired with FLIM, and the bottom, center and top bacterial planes were selected. Figure 2 shows that fluorescence lifetime also changes across bacterial height, and for *E. coli* it follows a similar trend as in eukaryotic cells increasing from 3.33 ns at the bottom to 3.75 ns at the top. In contrast, *B. subtilis* stained with Flipper-TR shows longer lifetimes at the top and the bottom, whereas a shorter lifetime is observed in the cell midplane (see also Figure S5). While the proximity to the glass interface could lead to a shorter fluorescence lifetime, since k_r is proportional to the square of the refractive index,[30] we ruled out this possibility by acquiring lifetime measurements of Rhodamine B near the surface and in solution (see Table S1). Therefore, we tentatively attribute the different trend in Gram positive

and negative bacteria to their cell wall structure, i.e. the former have a thick peptidoglycan layer, while the latter have a thinner peptidoglycan layer and an outer membrane.

Importantly, we performed as a control a similar experiment with the membrane dye Nile Red, a solvatochromic probe whose lifetime depends on the polarity of its molecular neighborhood and in turn on lipid packing, but has not been reported to depend on membrane tension.[31,32] The control experiment was performed in *B. subtilis*, which only has one membrane, to avoid issues with outer vs inner membrane localization of the fluorophore in *E. coli*. We first confirmed that Nile Red lifetime can be responsive to environmental differences in prokaryotic membranes (Figure S6). We note that using Nile Red lifetime as readout has limitations in eukaryotic cells due to its reduced sensitivity to cholesterol changes.[33] However, as opposed to eukaryotic membranes, prokaryotic membranes lack cholesterol and our data confirm that Nile Red is therefore a relevant solvatochromic control in these experiments.

Figure 2 shows that the lifetime of Nile Red only changes slightly, within the experimental uncertainty, across planes in *B. subtilis*. This result supports that Flipper-TR lifetime variations along bacterial height are mainly related to membrane tension, with potentially a small contribution due to changes in lipid composition (the latter has not been ruled out for eukaryotic cells[18]).

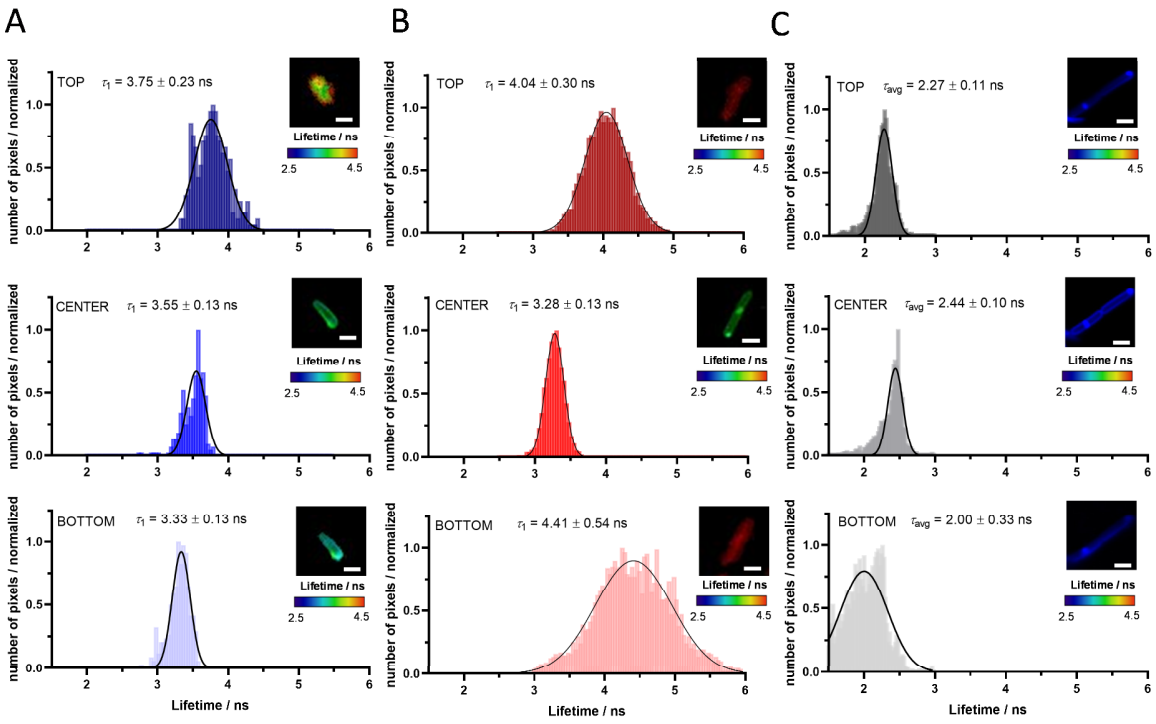

Figure 2. Fluorescence lifetime distributions at different Z planes of (A) *E. coli* stained with Flipper-TR (n = 63); (B) *B. subtilis* stained with Flipper-TR (n = 78); (C) *B. subtilis* stained with Nile Red (n = 27). All bacteria were immobilized on CellTak.

Flipper-TR is sensitive to bacterial-surface interaction

We next investigated if Flipper-TR can report on the interaction between bacteria and different surfaces. To that end, FLIM data of bacteria immobilized on glass coated with Poly-L-lysine (PLL) were compared to those on CellTak-coated glass. Since we observed Flipper-TR lifetime variations along the bacterial height, as reported in the previous section, the imaging plane in these experiments was as close as possible to the surface. Figure 3 shows the fluorescence lifetime histograms for both bacterial types on both surfaces. The lifetime values of bacteria

immobilized on PLL are shorter than on CellTak for both bacterial types, suggesting differences in the mode of interaction with the surface. Indeed, while bacterial interaction with PLL is mostly electrostatic, the adhesion mechanism of CellTak is dominated by the amino acid 3,4-dihydroxy-l-phenylalanine, which is formed by posttranslational modification of tyrosine, and presents multiple and complex adhesive roles.[34] The difference in Flipper-TR lifetime with the type of surface is much more pronounced for *B. subtilis* (0.67 ns) than for *E. coli* (0.13 ns). This is consistent with the observation that Flipper-TR stains the inner membrane in *E. coli*, as shown in the plasmolysis experiments. Indeed, outer membrane staining would likely result in a higher sensitivity of fluorescence lifetime to the surface type, which we do not observe.

A control FLIM experiment with Nile Red in *B. subtilis* (Figure 3) showed that this probe exhibits an almost identical average lifetime on both coated surfaces, PLL and CellTak. Therefore, the dependence of Flipper-TR lifetime with the surface mainly reflects a distinct physical interaction with each material. In other words, Flipper-TR is predominantly reporting differences in membrane tension rather than membrane composition upon bacterial interaction with each surface.

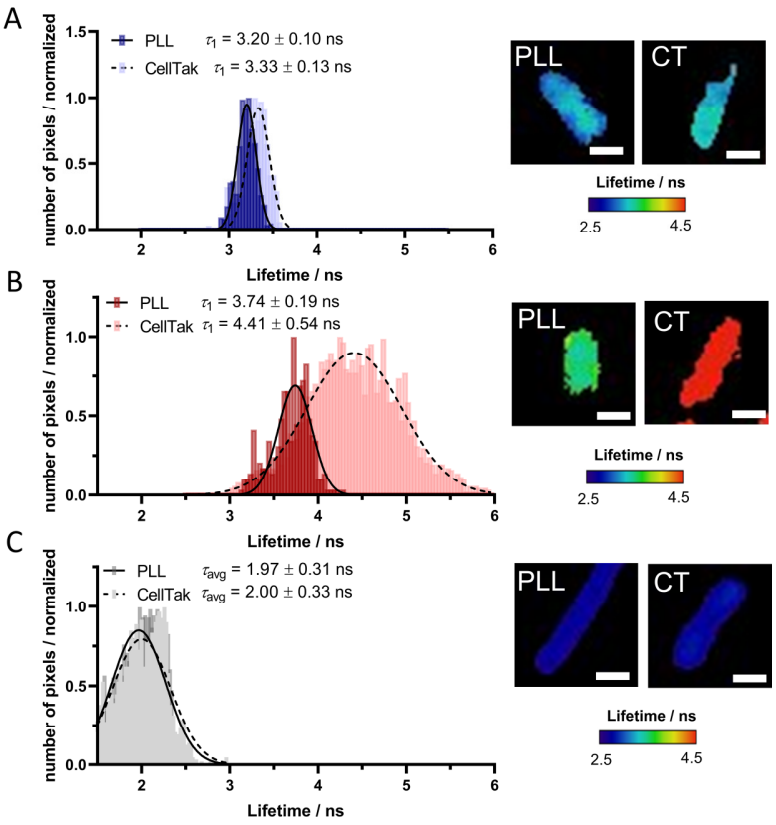

Figure 3. Fluorescence lifetime distributions and images at the bottom planes of bacteria immobilized on PLL and CellTak. (A) *E. coli* stained with Flipper-TR (n_{PLL}= 31, $n_{CellTak}$= 63); (B) *B. subtilis* stained with Flipper-TR (n_{PLL}= 18, $n_{CellTak}$= 78); (C) *B. subtilis* stained with Nile Red (n_{PLL}= 37, $n_{CellTak}$= 27). Average fluorescence lifetimes (τ_{avg}) are reported for Nile Red. The scale bar in the images is 2 µm.

Flipper-TR is sensitive to membrane tension induced by mechano-bactericidal topographies

To gain further insight into the sensitivity of Flipper-TR fluorescence lifetime to unravel bacterial-surface interactions, we next placed Flipper-TR-stained bacteria on a mechano-bactericidal polymer surfaces. The optically transparent UV-curable resin OrmoComp was used to fabricate the nanotopographies, allowing for good optical transparency during single-cell fluorescence microscopy, as we have previously shown.[11] The mechano-bactericidal topographies, which are bioinspired from the moth's eye, consisted of a well-defined array of nanocones with a nominal height of 350 nm, a width of 80 nm at the tip, and an aspect ratio of 4.3, arranged on a dense hexagonal lattice with a cone-to-cone distance of about 290 nm.[35] Nanocones with a 3-4 times lower aspect ratio were also fabricated (Figure S7). FLIM images on both nanofabricated surfaces were acquired and compared to that of bacteria on a flat surface of the same polymer. As in the previous section, the imaging plane was as close as possible to the surface. Figure 4 shows that the Flipper-TR fluorescence lifetime in *B. subtilis* on the flat polymer surface is 3.76 ns, and the average lifetime gradually decreases for low- (3.67 ns) and high-aspect-ratio nanocones (3.53 ns). Since bacterial interaction with these surfaces does not only include contact at the nanocone tips, but also stretching of the bacterial membrane suspended between nanocones,[36] we tentatively propose that the Flipper-TR lifetime in the stretched membrane regions (i.e. higher tensile stress) contributes to most of the fluorescence signal, resulting in an observable decrease in fluorescence lifetime. For reference, earlier studies in mammalian cells have shown a shorter Flipper-TR lifetime at the surface of nanopillars compared to the basal membrane.[37] While finite-element models can potentially assist in the interpretation of the FLIM data, current models have produced diverging results regarding the maximum points of stress/strain.[14]

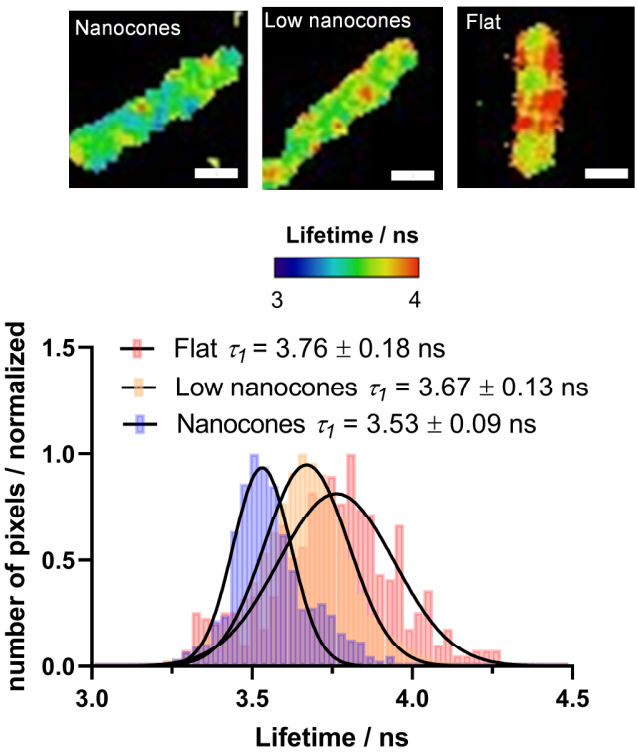

Figure 4. Fluorescence lifetime images and distributions at the bottom plane of *B. subtilis* stained with Flipper-TR on flat and nanosimprinted Ormocomp surfaces (n_{flat}= 13, n_{nanoc}= 12, n_{short}= 41). Scale bar is 2 µm.

CONCLUSIONS

In natural environments, bacteria are primarily found attached to surfaces rather than living as free-swimming cells. Therefore, bacteria-surface interactions are important to understand biofilm formation, or to engineer biomaterials with improved properties. However, few techniques are available to address this interface, and specifically the effects on membrane tension upon interaction of bacteria with surfaces. Indeed, mechanical stress modulates the function of proteins in the bacterial membrane, and has the potential to regulate multiple processes required for bacterial survival and growth.[38] Previous work indirectly determined

changes in bacterial membrane tension using a fluorescent Na^+ probe, since opening of mechanosensitive channels in the membrane leads to an increased ion flux.[8] As a more direct method, our study establishes the mechanosensitive fluorescent probe Flipper-TR and FLIM as a powerful tool to investigate bacterial membrane tension and interactions with material surfaces. We demonstrate that Flipper-TR effectively stains both Gram-positive and Gram-negative bacterial membranes, with fluorescence lifetime values that are shorter than those in eukaryotic cells and slightly vary between bacterial types, likely due to differences in membrane composition. The lifetimes of Flipper-TR vary along the vertical axis of the bacterial cell to a lesser extent than those of Nile Red, suggesting that this variation mainly corresponds to changes in membrane tension in a manner dependent on bacterial cell wall architecture.

Our findings show that Flipper-TR is sensitive to the nature of the bacterial-surface interaction. Bacteria on different adhesion-promoting coatings (PLL and CellTak) exhibit measurable differences in fluorescence lifetime, indicating variations in membrane tension driven by the mode of surface interaction. Moreover, Flipper-TR can detect membrane tension responses to engineered nanostructured surfaces. Bacteria interfacing with nanocone-patterned substrates displayed reduced Flipper-TR lifetimes compared to flat controls, which we attribute to the fluorescence signal being dominated by the stretched portion of the membrane between nanocones. These results highlight the sensitivity of Flipper-TR to biophysical forces at the cell-material interface and underscore its utility in elucidating bacterial responses to surface topography. Altogether, this work establishes a methodological foundation to study mechanical aspects of bacteria-surface interactions.

MATERIALS AND METHODS

Materials. Poly-L-lysine solution (PLL, Sigma-Aldrich), CellTak^{TM} (Corning), UV-curable resin OrmoComp (Microresist GmbH), Luria broth (Miller's broth) (Labkem), Luria agar (Miller's LB agar) (Labkem), and PBS (Sigma-Aldrich) were used as received. Fluorophores employed were Flipper-TR-TR probe (Spirochrome), Nile Red (Sigma Aldrich) and FM 4-64 (Thermofisher Scientific) and Rhodamine B (Sigma-Aldrich).

Bacterial cultures. *E. coli* BW25113 cells were grown overnight at 37°C in Miller LB medium (1% tryptone, 0.5% yeast extract, 1% NaCl). Overnight cultures were diluted 1:100 in fresh medium and grown to an optical density at 578 nm (OD578) of 0.4, and then diluted again to OD578 of 0.1, and grown to 0.4. *B. subtilis* 168 strain was grown overnight at 37°C in a Petri dish with in Miller LB agar medium. One bacterial colony was introduced in 10 mL of Miller LB medium and incubated at 37°C for 2.5 hours to obtain an OD578 of 0.4-0.6. 1 mL of cell culture (both *E. coli* and *B. subtilis*) was washed 3 times by centrifuging 3 min at 3000 x g and resuspending in a final volume of 0.5 mL of PBS to obtain bacterial suspensions.

Plasmolysis experiments. *E. coli* cells were grown as above. Cell samples were obtained and processed as published[39] with minor modifications. Briefly, 1.5 mL of cell culture were harvested (17,000 x g, 1 min), and pelleted cells were resuspended in 100 µl of plasmolysis solution (15% sucrose, 25 mM HEPES pH 7.4, 20 mM sodium azide). Fluorophores (FM 4-64 8.2 µM and Flipper-TR 2 µM) were added to the sample prior to immobilization of the cells in a 1% agarose pad (prepared using plasmolysis solution, as described.[29] Samples were visualized by confocal microscopy using a Leica Stellaris 8 with an excitation wavelength of 488 nm and

emission wavelength of 500-700 nm for Flipper-TR and an excitation wavelength of 500 nm and an emission wavelength of 600-800 for FM 4-64.

Surface preparation. Glass bottom Ibidi GmbH 35 mm diameter dishes were coated with PLL, CellTak, Ormocomp (Microresist Technology GmbH) film or patterned with nanocones. For PLL, 600 µL of PLL 1:10 were added to a dish and incubated for 15 minutes before washing with Mili-Q water and drying with nitrogen. CellTak coating was prepared adding 100 µL of a CellTak solution of 2.5 mg of CellTak in 1 mL of $NaHCO_3$ 0.1 M pH = 7, incubated for 1.5 hours, and then washed with Mili-Q water and dried with nitrogen. For the flat Ormocomp coating, Ibidi dishes were activated with O_2 plasma (Tepla, 150 ml/min) at 50 W during 2 minutes. Then a drop of a 150 mg/ml Ormocomp solution in toluene was added to the activated plate and spin-coated at 3000 rpm for 1 min. After that, the dish was cured under 80 mW/cm^2 UV light (UVASPOT 400/t, Honle) for 1 minute. Mechano-bactericidal topographies were fabricated with a PDMS moth-eye mold, as previously shown.[11,35,40] The mold was placed over a spincoated Ormocomp film, and left under 20 g weight for 2 minutes. The Ormocomp was then cured under a UV light as above. The template for low-aspect-ratio nanocones was obtained using the previously described roll-to-roll thermal nanoimprinting process,[41] in which PMMA moth-eye films were imprinted at 100 °C and produced at a web speed of 0.5 m/min. This substrate, used as a template, was replicated using two layers of polydimethylsiloxane (PDMS)[42] to obtain the working mold from which the Ormocomp nanocones were fabricated. The surface topography was characterized by atomic force microscopy (AFM) using a JPK/Bruker Nanowizard 5 in tapping mode with Tap300 GB-G probes (Budget Sensors, 300 kHz nominal resonance frequency, 40 N/m force constant).

Fluorescence Lifetime Imaging Microscopy. FLIM data were acquired on a Leica Stellaris 8 STED 3X with FLIM/FCS/DLS with a pulsed white-light laser (80 MHz, resulting in a 12.5 ns window) using a 63x water immersion objective with N.A.= 1.2. A phase element right before the objective lens was used to ensure circular polarization at the imaging plane. All images were acquired using 16 bits weight and 1024 x 1024 pixels with a pixel size of 45 nm x 45 nm. We used an excitation wavelength of 488 nm with 50% of intensity power. The emission was collected between 500 and 700 nm with a HyDX detector set to photon counting mode that discard the information containing more than 1 photon/count. Images were recorded using 1 Airy Unit which results in an optical section of 0.9 µm. The scan was run in bidirectional mode with a speed of 100 Hz with 16 line repetitions and 1 frame repetition with a pixel dwell time of 4.18 µs. Images were collected using Leica Application Suite LAS X FLIM/FCS software. The instrument response function (IRF) was obtained experimentally with erythrosine B dissolved in a saturated solution of KI.

For imaging, 1 µL of Flipper-TR or 5 µL Nile Red stock solution (1 mM) was added to 0.5 mL of bacterial suspension to a final concentration of 2 µM and 10 µM, respectively. For Flipper-TR, the sample was incubated at room temperature for 10 minutes. Then, a drop of 150 uL was added to the centre of the dish with the treated surface (PLL or CellTak) and incubated 10 minutes more before washing 3x with PBS to eliminate the excess of fluorophore and non-attached bacteria. Images were recorded at room temperature.

Fluorescence Lifetime Images Analysis. Images recorded by Leica Application Suite LAS X FLIM/FCS software were exported in .ptu format and analysed by the open software FLIMfit 5.1.1 (https://flimfit.org/downloads/5.1.1/). Images were fitted by a biexponential model following the equation (1) with a spatial binning of 4x4 pixels, a smoothing of 5 x 5 pixels (2

pixel radio) and 133 time bins of 97 ps/bin, obtaining decays of 10^3 – 10^4 photons (Figure S2). A minimum of 10^3 photons per decay are needed for biexponential fitting.[21,43]

$$I = I_0 + A_1 e^{-t/\tau_1} + A_2 e^{-t/\tau_2} \quad (1)$$

We refer to τ_1 as the longer lifetime, which is the one that reports on membrane tension. For deconvolution, the experimental IRF was employed. To select bacterial cells from the background we employed phasor plot segmentation with an intensity threshold of 1000 photons after binning.

Flipper-TR has two lifetimes and only the long lifetime reports on membrane tension (τ_1). Nile Red decays were also fitted to a biexponential model, since this fluorophore has complex excited-state dynamics, and in this case the average lifetime value is reported (τ_{avg}).[31] Bacterial autofluorescence decay was complex and also fitted with a biexponential model, reporting τ_{avg}.

ASSOCIATED CONTENT

Supporting Information. Autofluorescence analysis and plasmolysis experiments (Figures S1 and S2, respectively).

AUTHOR INFORMATION

Corresponding Author

*Correspondence should be addressed at cristina.flors@imdea.org.

Present address

[¶]Instituto de Estructura de la Materia, IEM-CSIC, C/Serrano, 121, Madrid, 28006 Spain.

Author Contributions

CF designed the project and wrote the paper, with contributions from all authors. MCGG and DB prepared bacterial samples and performed plasmolysis experiments, with the supervision of MP. MCGG acquired and analyzed FLIM images, with the support of JRI. MCGG fabricated surface nanotopographies with the help of JH and supervision of IR. All authors have given approval to the final version of the manuscript.

Funding Sources

This work was supported by the Spanish *Ministerio de Ciencia e Innovación* (MCIN/AEI / 10.13039/501100011033 / FEDER, UE), with grants PID2021-122231NB-I00 to CF, PID2020-120202RB-I00 to IR, PID2022-140818OA-I00 to MP, PID2021-125024NB-C21 to JRI, PRE2022-101502 to DB, CEX2021-001154-S, CEX2020-001039-S. Funding by the *Comunidad de Madrid* is also acknowledged: TecNanoBio-CM TEC-2024/TEC-158 to CF, 2020-T1/BMD-19970 to MP.

Notes

The authors declare no competing financial interest.

ACKNOWLEDGMENT

We thank Wilfried Meijer (Centro de Biología Molecular, Madrid) for the gift of *B. subtilis* 168, M. Alcaraz and F. Viela for preliminary FLIM experiments, and P. Pedraz at the IMDEA Nanociencia AFM service for topography measurements.

REFERENCES

(1) Tuson, H. H.; Weibel, D. B. Bacteria-surface interactions. *Soft Matter* **2013**, *9*, 4368-4380.

(2) Santore, M. M. Interplay of physico-chemical and mechanical bacteria-surface interactions with transport processes controls early biofilm growth: A review. *Adv Colloid Interface Sci* **2022**, *304*, 102665.

(3) Persat, A.; Nadell, C. D.; Kim, M. K.; Ingremeau, F.; Siryaporn, A.; Drescher, K.; Wingreen, N. S.; Bassler, B. L.; Gitai, Z.; Stone, H. A. The mechanical world of bacteria. *Cell* **2015**, *161*, 988-997.

(4) Carniello, V.; Peterson, B. W.; van der Mei, H. C.; Busscher, H. J. Physico-chemistry from initial bacterial adhesion to surface-programmed biofilm growth. *Adv Colloid Interface Sci* **2018**, *261*, 1-14.

(5) Huang, X.; Li, X.; Tay, A. Advances in techniques to characterize cell-nanomaterial interactions (CNI). *Nano Today* **2024**, *55*, 102149.

(6) Carniello, V.; Peterson, B. W.; Sjollema, J.; Busscher, H. J.; van der Mei, H. C. Surface enhanced fluorescence and nanoscopic cell wall deformation in adhering Staphylococcus aureus upon exposure to cell wall active and non-active antibiotics. *Nanoscale* **2018**, *10*, 11123-11133.

(7) Xu, Z.; Gamble, A.; Niu, W. A.; Smith, M. N.; Siegrist, M. S.; Tuominen, M.; Santore, M. M. Contact Area and Deformation of Escherichia coli Cells Adhered on a Cationic Surface. *Langmuir* **2023**, *39*, 6387-6398.

(8) Wang, L.; Wong, Y. C.; Correira, J. M.; Wancura, M.; Geiger, C. J.; Webster, S. S.; Touhami, A.; Butler, B. J.; O'Toole, G. A.; Langford, R. M.; Brown, K. A.; Dortdivanlioglu, B.; Webb, L.; Cosgriff-Hernandez, E.; Gordon, V. D. The accumulation and growth of Pseudomonas aeruginosa on surfaces is modulated by surface mechanics via cyclic-di-GMP signaling. *NPJ Biofilms Microbiomes* **2023**, *9*, 78.

(9) Liu, Y. N.; Liu, X. W. Nanoscale Spatiotemporal Dynamics of Microbial Adhesion: Unveiling Stepwise Transitions with Plasmonic Imaging. *ACS Nano* **2024**, *18*, 16002-16010.

(10) Liu, Y. N.; Lv, Z. T.; Lv, W. L.; Liu, X. W. Plasmonic probing of the adhesion strength of single microbial cells. *Proc Natl Acad Sci U S A* **2020**, *117*, 27148-27153.

(11) Viela, F.; Ortega, I. V.; Hernandez, J. J.; Rodriguez, I.; Moreno-Da Silva, S.; López-Moreno, A.; Pérez, E. M.; Flors, C. Real-Time Imaging of the Mechanobactericidal Action of Colloidal Nanomaterials and Nanostructured Topographies. *Small Sci.* **2023**, *3*, 2300002.

(12) Vadillo-Rodriguez, V.; Pedraz, P.; Flors, C. How Much Force is Needed to Kill a Single Bacterium? *Small* **2025**, *21*, e2407990.

(13) Del Valle, A.; Torra, J.; Bondia, P.; Tone, C. M.; Pedraz, P.; Vadillo-Rodriguez, V.; Flors, C. Mechanically Induced Bacterial Death Imaged in Real Time: A Simultaneous Nanoindentation and Fluorescence Microscopy Study. *ACS Appl Mater Interfaces* **2020**, *12*, 31235-31241.

(14) Baulin, V. A.; Linklater, D. P.; Juodkazis, S.; Ivanova, E. P. Exploring Broad-Spectrum Antimicrobial Nanotopographies: Implications for Bactericidal, Antifungal, and Virucidal Surface Design. *ACS Nano* **2025**, *19*, 12606-12625.

(15) Lin, N.; Berton, P.; Moraes, C.; Rogers, R. D.; Tufenkji, N. Nanodarts, nanoblades, and nanospikes: Mechano-bactericidal nanostructures and where to find them. *Adv Colloid Interface Sci* **2018**, *252*, 55-68.

(16) Linklater, D. P.; Baulin, V. A.; Juodkazis, S.; Crawford, R. J.; Stoodley, P.; Ivanova, E. P. Mechano-bactericidal actions of nanostructured surfaces. *Nat Rev Microbiol* **2021**, *19*, 8-22.

(17) Colom, A.; Derivery, E.; Soleimanpour, S.; Tomba, C.; Molin, M. D.; Sakai, N.; Gonzalez-Gaitan, M.; Matile, S.; Roux, A. A fluorescent membrane tension probe. *Nat Chem* **2018**, *10*, 1118-1125.

(18) Roffay, C.; Garcia-Arcos, J. M.; Chapuis, P.; Lopez-Andarias, J.; Schneider, F.; Colom, A.; Tomba, C.; Di Meglio, I.; Barrett, K.; Dunsing, V.; Matile, S.; Roux, A.; Mercier, V. Tutorial: fluorescence lifetime microscopy of membrane mechanosensitive Flipper probes. *Nat Protoc* **2024**, *19*, 3457.

(19) Chen, X. X.; Bayard, F.; Gonzalez-Sanchis, N.; Pamungkas, K. K. P.; Sakai, N.; Matile, S. Fluorescent Flippers: Small-Molecule Probes to Image Membrane Tension in Living Systems. *Angew Chem Int Ed Engl* **2023**, *62*, e202217868.

(20) Becker, W. Fluorescence lifetime imaging--techniques and applications. *J Microsc* **2012**, *247*, 119-136.

(21) Chang, C. W.; Sud, D.; Mycek, M. A. Fluorescence lifetime imaging microscopy. *Methods Cell Biol* **2007**, *81*, 495-524.

(22) Ragaller, F.; Sjule, E.; Urem, Y. B.; Schlegel, J.; El, R.; Urbancic, D.; Urbancic, I.; Blom, H.; Sezgin, E. Quantifying Fluorescence Lifetime Responsiveness of Environment-Sensitive Probes for Membrane Fluidity Measurements. *J Phys Chem B* **2024**, *128*, 2154-2167.

(23) Zuttion, F.; Colom, A.; Matile, S.; Farago, D.; Pompeo, F.; Kokavecz, J.; Galinier, A.; Sturgis, J.; Casuso, I. High-speed atomic force microscopy highlights new molecular mechanism of daptomycin action. *Nat Commun* **2020**, *11*, 6312.

(24) Valdivieso-González, D.; Sacristán, M. A.; Natale, P.; Orgaz, B.; Lillo, M. P.; Almendro-Vedia, V.; López-Montero, I. Elastic remodeling of model and cell membranes by rotating ATP synthase. *Cell Rep. Phys. Sci.* **2025**, *6*, 102567.

(25) Ramirez-Diaz, D. A.; Yin, L.; Albanesi, D.; Zheng, J.; de Mendoza, D.; Garner, E. C. The interplay of membrane tension and FtsZ filament condensation on the initiation and progression of cell division in B. subtilis. *bioRxiv* **2025**, *https://doi.org/10.1101/2025.05.18.654715*.

(26) Strahl, H.; Errington, J. Bacterial Membranes: Structure, Domains, and Function. *Annu Rev Microbiol* **2017**, *71*, 519-538.

(27) Nishibori, A.; Kusaka, J.; Hara, H.; Umeda, M.; Matsumoto, K. Phosphatidylethanolamine domains and localization of phospholipid synthases in Bacillus subtilis membranes. *J Bacteriol* **2005**, *187*, 2163-2174.

(28) While it has been previously suggested in reference 18 that Flipper-TR staining was unsuccessful in the Gram negative bacterium E. coli DH5α, showing only faint cytosolic signal, we note that we are using a different strain.

(29) Ginez, L. D.; Osorio, A.; Vazquez-Ramirez, R.; Arenas, T.; Mendoza, L.; Camarena, L.; Poggio, S. Changes in fluidity of the E. coli outer membrane in response to temperature, divalent cations and polymyxin-B show two different mechanisms of membrane fluidity adaptation. *Febs J* **2022**, *289*, 3550-3567.

(30) Lakowicz, J. R.: *Principles of Fluorescence spectroscopy*; 2nd ed.; Kluwer Academic: New York, 1999.

(31) Levitt, J. A.; Chung, P. H.; Suhling, K. Spectrally resolved fluorescence lifetime imaging of Nile red for measurements of intracellular polarity. *J Biomed Opt* **2015**, *20*, 096002.

(32) Lira, R. B.; Dillingh, L. S.; Schuringa, J. J.; Yahioglu, G.; Suhling, K.; Roos, W. H. Fluorescence lifetime imaging microscopy of flexible and rigid dyes probes the biophysical properties of synthetic and biological membranes. *Biophys J* **2024**, *123*, 1592-1609.

(33) Mukherjee, S.; Raghuraman, H.; Chattopadhyay, A. Membrane localization and dynamics of Nile Red: effect of cholesterol. *Biochim Biophys Acta* **2007**, *1768*, 59-66.

(34) Lee, H.; Scherer, N. F.; Messersmith, P. B. Single-molecule mechanics of mussel adhesion. *Proc Natl Acad Sci U S A* **2006**, *103*, 12999-13003.

(35) Viela, F.; Navarro-Baena, I.; Hernandez, J. J.; Osorio, M. R.; Rodriguez, I. Moth-eye mimetic cytocompatible bactericidal nanotopography: a convergent design. *Bioinspir Biomim* **2018**, *13*, 026011.

(36) Pogodin, S.; Hasan, J.; Baulin, V. A.; Webb, H. K.; Truong, V. K.; Phong Nguyen, T. H.; Boshkovikj, V.; Fluke, C. J.; Watson, G. S.; Watson, J. A.; Crawford, R. J.; Ivanova, E. P. Biophysical model of bacterial cell interactions with nanopatterned cicada wing surfaces. *Biophys J* **2013**, *104*, 835-840.

(37) Sansen, T.; Sanchez-Fuentes, D.; Rathar, R.; Colom-Diego, A.; El Alaoui, F.; Viaud, J.; Macchione, M.; de Rossi, S.; Matile, S.; Gaudin, R.; Backer, V.; Carretero-Genevrier, A.; Picas, L. Mapping Cell Membrane Organization and Dynamics Using Soft Nanoimprint Lithography. *ACS Appl Mater Interfaces* **2020**, *12*, 29000-29012.

(38) Genova, L. A.; Roberts, M. F.; Wong, Y. C.; Harper, C. E.; Santiago, A. G.; Fu, B.; Srivastava, A.; Jung, W.; Wang, L. M.; Krzeminski, L.; Mao, X.; Sun, X.; Hui, C. Y.; Chen, P.; Hernandez, C. J. Mechanical stress compromises multicomponent efflux complexes in bacteria. *Proc Natl Acad Sci U S A* **2019**, *116*, 25462-25467.

(39) Nilsson, I.; Six, D. A. Metabolic Incorporation of Azido-Sugars into LPS to Enable Live-Cell Fluorescence Imaging. *Methods Mol Biol* **2022**, *2548*, 267-278.

(40) Navarro-Baena, I.; Jacobo-Martin, A.; Hernandez, J. J.; Castro Smirnov, J. R.; Viela, F.; Monclus, M. A.; Osorio, M. R.; Molina-Aldareguia, J. M.; Rodriguez, I. Single-imprint moth-eye anti-reflective and self-cleaning film with enhanced resistance. *Nanoscale* **2018**, *10*, 15496-15504.

(41) Jacobo-Martin, A.; Rueda, M.; Hernandez, J. J.; Navarro-Baena, I.; Monclus, M. A.; Molina-Aldareguia, J. M.; Rodriguez, I. Bioinspired antireflective flexible films with optimized mechanical resistance fabricated by roll to roll thermal nanoimprint. *Sci Rep* **2021**, *11*, 2419.

(42) Jacobo, A.; Hernández, J. J.; Pedraz, P.; Solano, E.; Navarro-Baena, I.; Rodriguez, I. Improved thermal stability of antireflective moth-eye topography imprinted on PMMA/TiO<u>2</u> surface nanocomposites. *Nanotechnology* **2021**.

(43) Luchtefeld, I.; Pivkin, I. V.; Gardini, L.; Zare-Eelanjegh, E.; Gabelein, C.; Ihle, S. J.; Reichmuth, A. M.; Capitanio, M.; Martinac, B.; Zambelli, T.; Vassalli, M. Dissecting cell membrane tension dynamics and its effect on Piezo1-mediated cellular mechanosensitivity using force-controlled nanopipettes. *Nat Methods* **2024**, *21*, 1063-1073.